

Shape Biased Low Power Spin Dependent Tunneling Magnetic Field Sensors

10-5-2001

Mark Tondra, Zhenghong Qian, Dexin Wang, Cathy Nordman, John Anderson, Albrecht Jander,
Bob Sinclair, James Daughton
NVE Corporation
11409 Valley View Road, Eden Prairie, MN 55344

ABSTRACT

Spin Dependent Tunneling (SDT) devices are leading candidates for inclusion in a number of Unattended Ground Sensor applications. Continued progress at NVE has pushed their performance to 100s of pT / rt. Hz @ 1 Hz. However, these sensors were designed to use an applied field from an on-chip coil to create an appropriate magnetic sensing configuration. The power required to generate this field (~100mW) is significantly greater than the power budget (~1mW) for a magnetic sensor in an Unattended Ground Sensor (UGS) application. Consequently, a new approach to creating an ideal sensing environment is required.

One approach being used at NVE is “shape biasing.” This means that the physical layout of the SDT sensing elements is such that the magnetization of the sensing film is correct even when no biasing field is applied. Sensors have been fabricated using this technique and show reasonable promise for UGS applications. Some performance trade-offs exist. The power is easily under 1 mW, but the sensitivity is typically lower by a factor of 10. This talk will discuss some of the design details of these sensors as well as their expected ultimate performance.

1. Introduction and Motivation

SDT sensors are the most advanced of all magnetoresistive magnetic field sensors. Significant effort is being expended to adapt them to the UGS application. The motivation for this effort is the expectation that SDT sensors will offer the best combination of parameters of interest for the UGS concept: high sensitivity, low power, tiny package, low cost for large quantities, and ease of use and integration.

Reducing the required operating power is one of the biggest challenges in the SDT development (reducing low frequency noise is the other). Though the SDT sensor bridges can be made to have a very high resistance (correspondingly low intrinsic power) they presently require a magnetic field bias that uses more than 100 mW to generate. The bridge itself typically requires less than 1 mW. This paper will discuss some of the options being explored in the effort to eliminate the need for the field bias. It will discuss in detail a specific design that employs magnetic “shape biasing” to do so.

Report Documentation Page

Report Date 05OCT2001	Report Type N/A	Dates Covered (from... to) -
Title and Subtitle Shape Biased Low Power Spin Dependent Tunneling Magnetic Field Sensors	Contract Number	
	Grant Number	
	Program Element Number	
Author(s)	Project Number	
	Task Number	
	Work Unit Number	
Performing Organization Name(s) and Address(es) NVE Corporation 11409 Valley View Road Eden Prairie, MN 55344	Performing Organization Report Number	
Sponsoring/Monitoring Agency Name(s) and Address(es)	Sponsor/Monitor's Acronym(s)	
	Sponsor/Monitor's Report Number(s)	
Distribution/Availability Statement Approved for public release, distribution unlimited		
Supplementary Notes Papers from 2001 Meeting of the MSS Specialty Group on Battlefield Acoustic and Seismic Sensing, Magnetic and Electric Field Sensors, Volume 1: Special Session held 23 Oct 2001. See also ADM001434 for whole conference on cd-rom., The original document contains color images.		
Abstract		
Subject Terms		
Report Classification unclassified	Classification of this page unclassified	
Classification of Abstract unclassified	Limitation of Abstract UU	
Number of Pages 8		

1.1. UGS Operational Requirements

The Unattended Ground Sensors concept is assumed to be, in this paper, an array of sensor modules distributed about a field. The modules would communicate using RF, and be battery powered. Each module would contain system control and data processing devices that are shared amongst the many sensors on board. Sensor types could include seismic, acoustic, and electric field, as well as magnetic field transducers. Presumably, the batteries would need to last for a month or so. Batteries will occupy a considerable fraction of the total available space. The space would be on the order of a few 100 cubic cm, or about the size of a closed fist.

1.2. Magnetic Field Sensor Power and Volume Budget

The concept is still evolving, so some reasonable estimates of the power and space allocations will have to be made. Thus, a power budget of 1 mW at 3.3 Volts is allocated to the magnetic field sensor component of an UGS module. Furthermore, the allowed volume will be the size of an 8 pin SOIC chip for each of three orthogonal axes. The total volume of a three-axis magnetic field sensor will be about 1 cc. This power and volume budget includes the magnetic transducer alone, and not any signal conditioning, processing, or control circuitry.

1.3. Magnetic Field Sensor Noise Floor Requirements

The noise floor of the sensor is also an extremely important parameter. If the sensor is not sensitive enough, the magnetic field sensor could be the limiting factor for how closely spaced the UGS modules must be. Ideally, the communications range will be the limit. For most envisioned systems, the sensor noise floor must be better than 1 nT / rt. Hz at 1 Hz. A preferred value would be 1 pT / rt. Hz. (1 nTesla = 1×10^{-5} Gauss). Though this paper will not discuss noise issues in detail, some attempt will be made to point out how power and sensitivity may be traded off against one another.

2. Magnetic Design Details

In nearly all linear magnetoresistive field sensors, the magnetic design objective is to force the magnetization of the sensing film to rotate smoothly in response to variations in the measured field. In the case of SDT sensors, the resistance varies as the (-) cosine of the angle between the magnetizations of thin ferromagnetic films on either side of a tunnel barrier.

$$R = R_0 - (\Delta R / 2)(\cos \theta) \tag{1}$$

This equation describes the resistance of the SDT device only to the extent that the magnetizations are oriented in a uniform and well defined way. Any non-uniformity or irregularity leads to more complicated and less desirable operation.

One can see from equation (1) that the intermediate value of the SDT resistance occurs at $\theta = 90^\circ$. Thus a bipolar sensor output can be created if the following situation is created: The magnetizations are perpendicular when no external field is applied, and they become more antiparallel (parallel) as a positive (negative) field is applied. If one of the magnetizations is fixed ("pinned" layer), the situation is fairly simple, and the resistance is wholly dependent on the orientation of the other magnetization ("free" layer). From this point on, "pinned layer" and "free layer" will refer to the orientation of the respective magnetizations of those layers. Figure 1 below shows the resistance of a hypothetical device where one layer rotates from parallel to antiparallel in an applied field that sweeps from negative to positive.

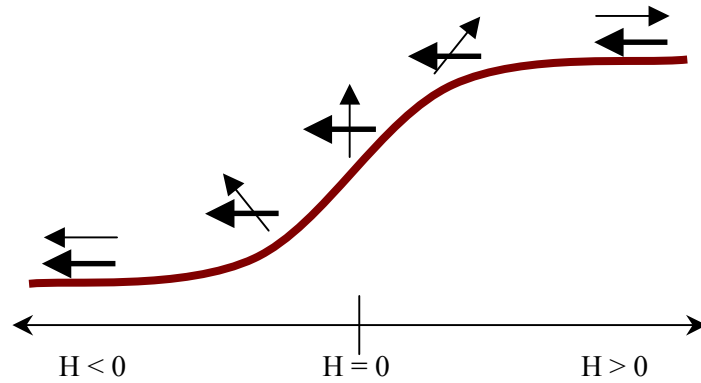


Figure 1: A representation of the SDT resistance as a function of externally applied field. The thick and thin arrows represent the pinned and free layers, respectively.

In previous versions of the SDT sensors, an applied magnetic field was used to cause the free layer to be perpendicular to the pinned layer at $H = 0$. In the sensor discussed in this paper, the perpendicular configuration is achieved through other means called “shape biasing.” In addition to using shape, the “easy axis” of the free layer was made to be perpendicular to the pinned layer. These two tools together were required to achieve good sensing behavior in the free layer.

Shape biasing is a phrase that encompasses the fact that the magnetization prefers to be oriented along the longest dimension of an object. Consider a long, narrow thin film device (say $100\mu\text{m} \times 2\mu\text{m} \times 0.01\mu\text{m}$). The magnetization is very difficult to rotate out of the plane, and will be mostly oriented along the long axis. The aspect ratio of this film ($100 : 2 = 50 : 1$) is quite large. The magnitude of the shape bias effect is roughly proportional to the aspect ratio.

3. Sensor Construction

The shape biased sensor designs under development at this time have an aspect ratio of $15 : 1$ for the sensing film. The widths of the sensing layers for these three designs are $2\mu\text{m}$, $6\mu\text{m}$, and $10\mu\text{m}$. SDT Layers. The layers in the SDT stack are NiFeCo 125 / Al_2O_3 15 / FeCo 50 / Ru 9 / FeCo 50 / CrPtMn 300 (in Angstroms). The free layer (bottom) is deposited in a 20 Gauss field such that its easy axis is perpendicular to the sensing direction. The pinned layer is also oriented in this direction initially, but is rotated to be parallel to the sensing direction in subsequent processing steps.

3.1. Patterning

The SDT devices are patterned from the blank SDT film in a two-etch process. The top electrodes are defined first, then the bottom electrodes. The patterns are such that the aspect ratio of the bottom electrodes is $15 : 1$. The width of the bottom electrode is 2, 4, or 10 microns, depending upon which variation is being used. Figure 2 gives a general idea of what individual patterned SDT devices look like.

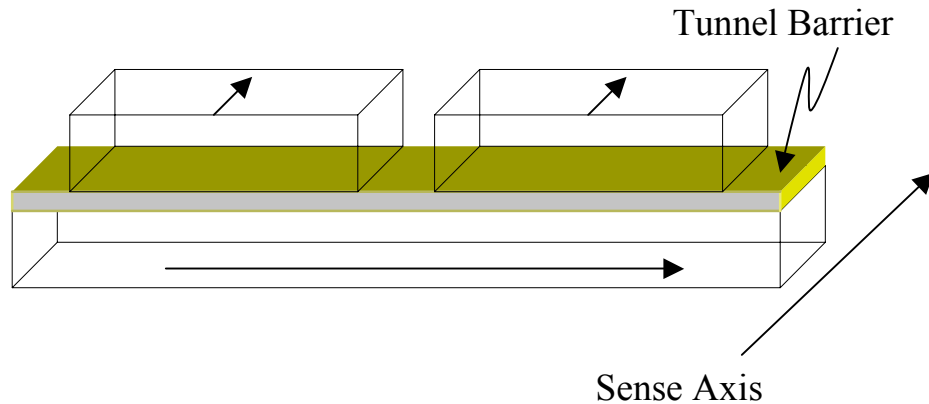


Figure 2: A representation of one pair of shape biased SDT elements. Two SDT elements share a common bottom sensing film. The arrows in the top regions indicate the orientation of the magnetization of the pinned layers. The arrow in the bottom indicates the easy axis of the free layer.

3.2. Bridge Design

The pairs of junctions shown above are a small part of an entire sensor. The whole sensor is configured as a Wheatstone bridge. Each leg of the bridge has many tunnel junctions connected together. The present project is using three designs on the same lithography mask set. Each of the three bridge designs has the same total area containing tunnel junctions. They are in a region about $60\ \mu\text{m} \times 600\ \mu\text{m}$, in the gap between two flux concentrators. More junctions can fit into the same area if they are small, fewer if they are large. The three designs have the following junction setup: 1) 30 junctions per leg with area = $420\ \mu\text{m}^2$; 2) 60 junctions per leg with area = $160\ \mu\text{m}^2$; and 3) 216 junctions per leg with area = $24\ \mu\text{m}^2$.

3.3. Annealing

Creating an ideal sensing film requires more than proper geometrical design. Annealing steps must be performed to set the direction of the pinned layer, improve the magnetic uniformity of the sensing layer, and improve the tunneling properties of the insulating barrier.

A post-deposition anneal is performed perpendicular to the sensing direction in order to enhance the stability of the free layer easy axis and reduce dispersion. Once the junctions are patterned, a second anneal is performed with a field applied perpendicular to the sensing direction to enhance the properties of the sensing layer. A final anneal is performed with the field parallel to the sense direction. This last anneal reorients the pinning direction and results in the desired orthogonal sensing configuration. The present process calls for one hour at $250\ ^\circ\text{C}$ in $2400\ \text{Oe}$ for the first and second anneals. Considerable improvement in the magnetic and magnetoresistive properties is expected with continued refinement of the annealing procedures.

4. Results

Good results have been achieved using these fabrication techniques. Data from two sensor bridges are shown below in Figures 3 through 5. These bridges do not yet have flux concentrators, so the finished sensor output will have a significantly higher (about 7x) slope than shown here.

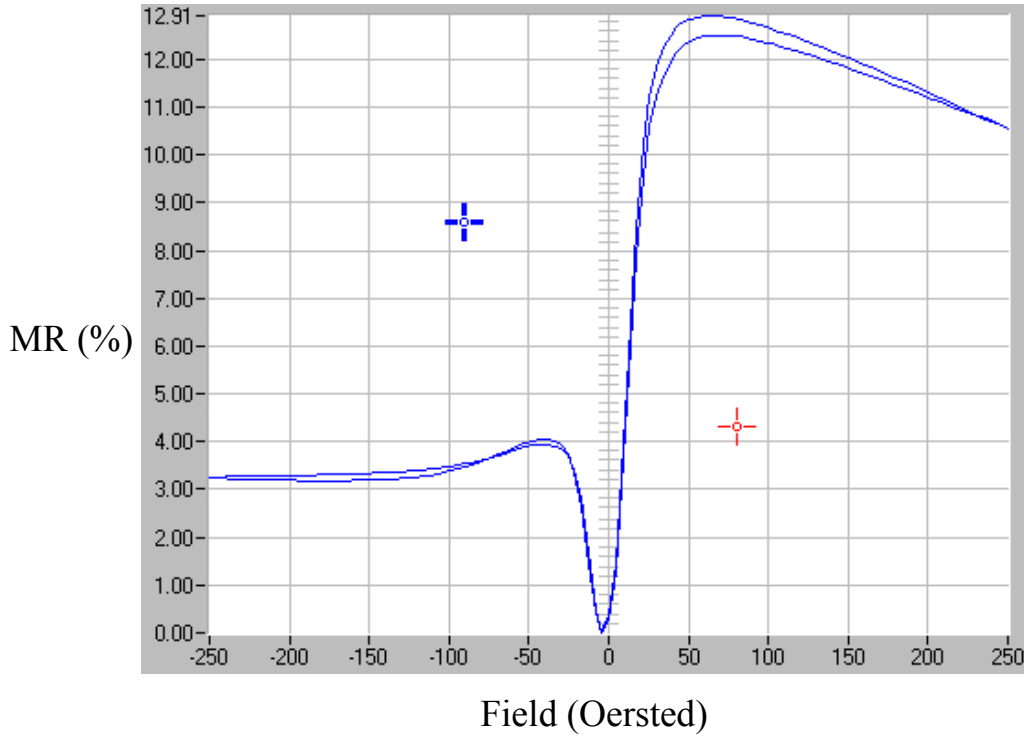


Figure 3: A two-terminal measurement of the resistance of a shape-biased SDT sensor. The useful sensing region is from ~ -5 Oe to $\sim +20$ Oe. These junctions have $10 \mu\text{m} \times 150 \mu\text{m}$ bottom electrodes and $6 \mu\text{m} \times 70 \mu\text{m}$ top electrodes (area = $420 \mu\text{m}^2$). The resistance of each junction is approximately 1 kOhm, and the resistance area product (RAP) = $420 \text{ kOhm} \cdot \mu\text{m}^2$.

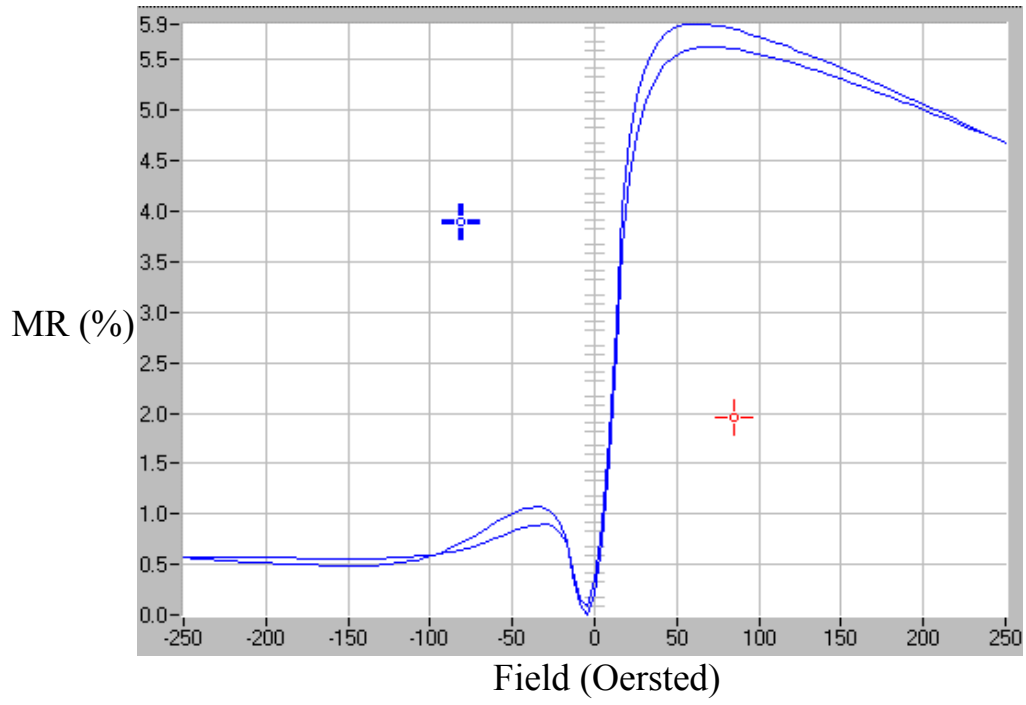


Figure 4: A wide field sweep of the resistance of another shape biased tunnel junction.

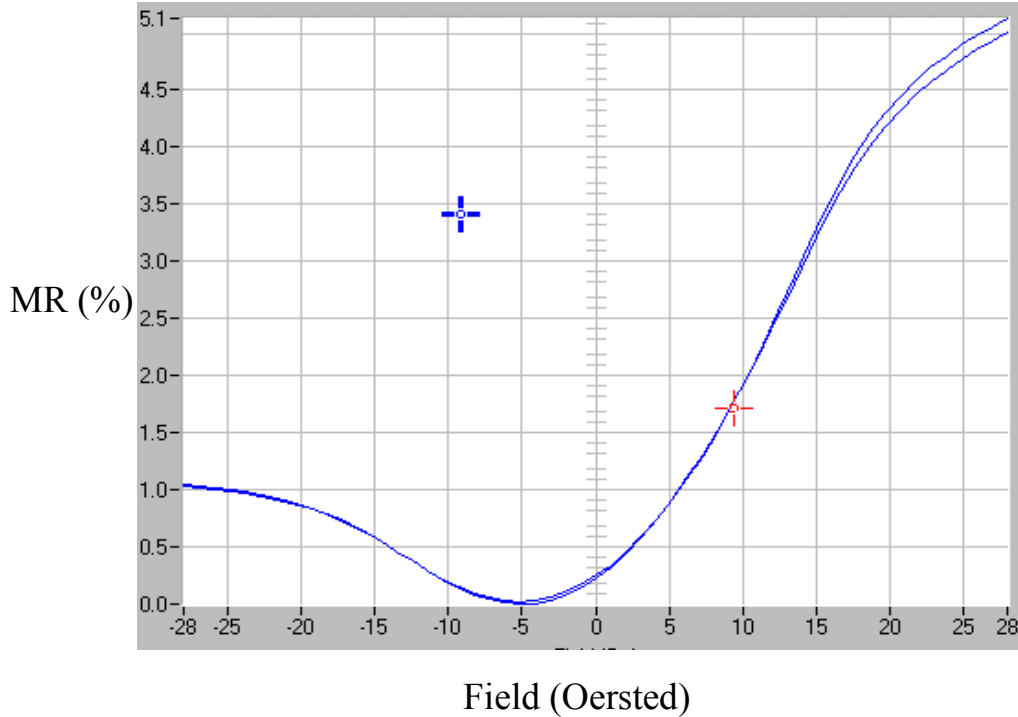


Figure 5: The same bridge as in Figure 4, but in a narrower field range. The hysteresis is virtually zero in the range of 1 to 12 Oe.

The nonhysteretic output of these bridges is very promising. The magnetoresistance can be improved significantly. It is not directly related to the shape of the output, but only the amplitude. There are two areas that need improvement in terms of magnetic behavior. The first is improved magnetoresistance. There is no reason it can't be better than 40%. The second area for improvement is the shift of the “sweet spot” of the output. Ideally, it would be at zero field rather than shifted to +5 Oe as is the case in the data here. This shift is due to magnetic coupling across the tunnel barrier, and imperfect orientation of the easy axis of the free layer and pinned layer.

5. Discussion and Conclusions

5.1. Power

The power required to run these bridges depends on a number of issues. The bridge power is simply V^2 / R , where V is the voltage and R is the resistance. V is typically fixed at a value like 3 volts. R , however, depends on the bridge configuration and the Resistance-Area Product (RAP).

$$R = (\# \text{ junctions per leg}) \times (\text{resistance} / \text{junction}) = (\# \text{ per leg}) \times (\text{RAP} / \text{junction area}) \quad (2)$$

Given a typical RAP of $1 \text{ M}\Omega\text{-}\mu\text{m}^2$ and voltage of 3V, the three bridge designs draw $4.2 \mu\text{W}$,

400 nW, and 6 nW, respectively. A RAP of $100 \text{ k}\Omega\text{-}\mu\text{m}^2$ at the same voltage would still result in a $42 \mu\text{W}$ draw at most. These numbers are clearly within the power budget stated at the beginning of this paper.

The sensitivity of finished sensors using the bridges described above will be about 7x that shown here due to the flux concentrators. When operated at 3 Volts, the signal will range from 50 mV / Oe to 500 mV / Oe, depending upon the magnetoresistance and quality of a given sensor.

5.2. Noise

The noise of these high impedance bridges may be of concern. Consider the most resistive case. The resistance of the 6 nW sensor listed above is 9 MOhms. The thermal (also known as Johnson) noise for this resistance is about 400 nV / rt. Hz. Assuming a sensitivity of 400 mV / Oe, the minimum detectable field is (noise / sensitivity) = $1 \mu\text{Oe}$ / rt. Hz. It remains to be seen how much of a 1/f noise contribution there is at low frequencies in these sensors. However, one should note that the current will be quite low. Thus, there may be less than a factor of ten excess noise at 1 Hz above the high frequency limit.

In the case of the $4.2 \mu\text{W}$ sensor, the resistance is about 70 k Ω , and the corresponding thermal noise is 34 nV / rt. Hz. Making the same assumptions about sensitivity, the thermal noise floor of this sensor would be 10's of pT / rt. Hz. Again, the 1/f component is not yet known.

5.3. Conclusion

The results shown here demonstrate that shape biasing can be used to generate a non-hysteretic output in an SDT sensor bridge without the use of an additional field bias. The thermal noise floor for typical values of resistance would range from 10's to 100's of pT / rt. Hz. This is still in the range of interest for the UGS application, and has the benefit of not requiring any field biasing. Because the basic bridge sensor design is the same as previous versions, these sensors can be dropped directly into circuitry designed for the field-biased SDT sensors.

6. Acknowledgements

This work was largely funded by SBIR contracts with the US Army and US Air Force. Many thanks also to John Taylor and Seraphin Akou for their work on testing the devices.

7. References

1. M. Tondra, SPIE conference April 2001, Orlando, Florida. Proceedings in press.
2. B. Schrag, A. Anguelouch, G. Xiao, P. Trouilloud, T. Lu, W. Gallagher, and S.S.P. Parkin, J. Appl. Phys., 87, 4682 (2000).
3. S. Mao, J. Giusti, N. Amin, J. Van Ek, and E. Murdock, J. Appl. Phys., 85, 6112 (1999).
4. K. Moon, R. Fontana, and S.S.P. Parkin, J. Appl. Phys., 74, 3690 (1999).